UCSD IGPJEFF-FNL

Earthquake Activity near Ascension Island as seen by a Combined Seismic/Hydrophone Array

Final Report
February 1 1993 - February 28, 1996

Principal Investigator:
Holly K. Given
Institute of Geophysics and Planetary Physics
Scripps Institution of Oceanography
University of California, San Diego
9500 Gilman Drive
La Jolla, CA 92093-0225

Sponsored by
Advanced Research Projects Agency
Nuclear Monitoring Research Office
ARPA Order No. 6502 Program Code No. 1A10
Issued by ARPA/CMO under Contract #MDA972-91-C-0005

REPORT DOCUMENTATION PAGE

Form Approved
OMB No. 0704-0188

1. AGENCY USE ONLY *(Leave blank)*

2. REPORT DATE
02/28/96

3. REPORT TYPE AND DATES COVERED
Final Technical Report, ending 02/28/96

4. TITLE AND SUBTITLE
Earthquake Activity Near Ascension Island as Seen by a Combined Seismic/ Hydrophone Array; Final Report

5. FUNDING NUMBERS
Program Code No. 1A10
ARPA Order No. 6502
Contract # MDA972-91-C-0005

6. AUTHOR(S)
Holly K. Given, Jeff A. Hanson, Jonathan Berger

7. PERFORMING ORGANIZATION NAME(S) AND ADDRESS(ES)
The Regents of the University of California
Scripps Institution of Oceanography
IGPP 0225, 9500 Gilman Drive
La Jolla, California 92093-0225

8. PERFORMING ORGANIZATION REPORT NUMBER

9. SPONSORING/MONITORING AGENCY NAME(S) AND ADDRESS(ES)
Advanced Research Projects Agency
3701 North Fairfax Drive
Arlington VA 22203-1714

10. SPONSORING /MONITORING AGENCY REPORT NUMBER

11. SUPPLEMENTARY NOTES
Final report on AASERT (Augmentation Awards for Science and Engeering Research Training) supplement/extension to parent grant MDA972-91-C-0005. Preprint of paper to appear in Geothermics, special issue on Ascension Island.

12a. DISTRIBUTION/AVAILABILITY STATEMENT

12b. DISTRIBUTION CODE

13. ABSTRACT *(Maximum 200 words)*

Data from a recently installed Global Seismographic Network station on Ascension Island in the central Atlantic Ocean (IRIS/IDA ASCN) are used in conjunction with data from a network of ocean hydrophones (MILS network) deployed around the island to detect and locate background seismicity associated with the mid-Atlantic Ridge and nearby tranform faults. Locations calculated from the combined data set have errors less than 10 km, and frequently less than 3 km. A local magnitude scale based on S-wave amplitudes at the seismic station is devised. We estimate a detection threshhold of about magnitude 1.7 for earthquakes occurring on the nearby part of the ridge, 120 km away; this is almost three orders of magnitude smaller than the smallest events from this region in the PDE or REB catalogs. No natural seismicity on Ascension Island itself was seen during a 200-day observation period. The seismic station regularly records large T-phases from moderate-sized events around the Atlantic. T-phases are more pronounced at IRIS/IDA station SHEL on St. Helena Island, 1290 km southeast of Ascension Island, probably due to its steeper topography. Taken together, the seismic stations ASCN, SHEL, and the MILS network represent a unique facility to monitor seismic events in the south Atlantic.

14. SUBJECT TERMS
seismicity, detection, hydroacoustic, Ascension Island

15. NUMBER OF PAGES

16. PRICE CODE

17. SECURITY CLASSIFICATION OF REPORT	18. SECURITY CLASSIFICATION OF THIS PAGE	19. SECURITY CLASSIFICATION OF ABSTRACT	20. LIMITATION OF ABSTRACT
Unclassified	Unclassified	Unclassified	SAR

NSN 7540-01-280-5500

Standard Form 298 (Rev 2-89)
Prescribed by ANSI Std. 239-18
298-102

Earthquake Activity Near Ascension Island as seen by a Combined Seismic/Hydrophone Array

Jeff A. Hanson, Holly K. Given, and Jonathan Berger
Institute of Geophysics and Planetary Physics
Scripps Institution of Oceanography
University of California, San Diego
La Jolla, California 92093

Submitted to Geothermics (special edition on Ascension Island) August 24, 1995

Revised February 1, 1996.

Earthquake Activity Near Ascension Island as seen by a Combined Seismic/Hydrophone Array

Jeff A. Hanson, Holly K. Given, and Jonathan Berger
Institute of Geophysics and Planetary Physics
Scripps Institution of Oceanography
University of California, San Diego
La Jolla, California 92093

Abstract

Earthquake activity in the vicinity of Ascension Island is studied using data from a recently installed, very broadband seismographic station and a network of ocean hydrophones deployed around the island. The seismic station ASCN recorded 121 local earthquakes over a 188 day period. Distance from ASCN is computed for 41 of these events, most of which occurred at approximately 100 km - the distance to the Mid-Atlantic Ridge. A local magnitude scale is calibrated and applied to the same 41 events with magnitudes ranging from 0.4 to 4.2. Six earthquakes were located using data from the hydrophones and ASCN. Two of the earthquakes occur on the Ascension Fracture Zone 35 km northwest of the island and the other four near the ridge-transform intersection. The locations have errors less than 10 km and frequently less than 3 km. There is no direct evidence for seismicity connected with geothermal activity on Ascension Island during the observation period.

Key words: microearthquakes, mid-ocean ridge, fracture zone, Ascension Island.

Introduction

Ascension Island is located in the middle of the Atlantic Ocean 8 degrees south of the equator (Fig. 1). It lies just 100 km from the Mid-Atlantic Ridge (MAR), making it one of the closest landmasses to an active, oceanic spreading center. In general, seismic activity is usually observed in conjunction with known geothermal areas (e. g. Romero *et al.*, 1995), but little is known about the seismicity of Ascension Island. In October of 1994 a broadband seismic station (ASCN), as part of the IRIS/IDA Global Seismographic Network, was installed on the island near Butt Crater. The station is unique in several aspects. With a few exceptions, ridge microseismicity studies have used Ocean Bottom Seismometers (OBS) which, unlike ASCN, are not usually broadband and have only been deployed for short periods of time (less than 6 months). In addition, there is a hydrophone array that surrounds Ascension Island run by the U.S. Air Force (Palmer *et al.*, 1994). In this study ASCN in combination with the hydrophones is used as a mini-network to locate earthquakes and make a preliminary quantification of the local seismicity around Ascension Island with the first 188 days of data.

Ascension is a recent volcanic island with rocks dating from approximately 1.5 Ma to 700 years ago (Atkins *et al.*, 1969; Baker, 1973). It is clear that there is extra magma activity in the area due to the Ascension Hotspot (O'Connor and le Roex, 1992), but the present day location of the hotspot is not obvious. It was originally proposed that Ascension Island itself marked the current position (Burke and Wilson, 1976; Morgan 1971), but since then a detailed magnetic anomaly study of the area has placed the hotspot just east of the ridge, a few degrees southeast of Ascension (Brozena, 1986). Brozena argues that the hotspot feeds magma into the MAR, and the magma runs north along the ridge until it reaches the Ascension Fracture Zone (due to a major offset in the MAR). Because of the relatively cold material it encounters there, the magma pools

and spreads out just south of the fracture zone. This causes magma extrusions such as Ascension Island and a chain of seamounts running perpendicular to the ridge. This addition of heat will change the extent of brittle lithosphere, and thus the seismicity of the area can be used to test such hypotheses about ridge dynamics, crustal variations, and magma sources.

Earthquakes larger than magnitude 4.5 associated with the MAR and the fracture zones are recorded by global seismic networks and reported in catalogs such as the Preliminary Determination of Epicenters (PDE), however, most of the smaller earthquakes go unreported. The PDE catalog records earthquake parameters such as epicenter coordinates, depth, origin times and magnitudes. Earthquakes with magnitudes greater than 6.0 are not seen on ridge segments (Huang *et al.*, 1986), but they are seen occasionally on transform faults (Bergman and Solomon, 1988). Therefore the global catalogs only record southern Atlantic earthquakes in the magnitude range 4.5 and 6.0 and many potentially interesting events go unobserved.

Most of the seismicity in the Atlantic occurs on the MAR or along its associated transform faults. The MAR is a slow-to-medium rate spreading center with a full spreading rate of ~35 mm/yr. (Cande *et al.*, 1988). The seismicity on the ridge tends to be extensional faulting, while transform faults produce strike-slip earthquakes. The ridge is broken up into major segments which are about 200 to 500 km long and are offset by large transform faults that are as long as 300 km. On the MAR these major segments are also broken up into many small segments with small offsets. The large offset transform faults leave deep valleys in the crust known as fracture zones that extend perpendicular to the ridge axis, and just 30 km north of Ascension Island is one such valley known as the Ascension Fracture Zone (AFZ) (van Andel *et al.*, 1973). The AFZ, along with other fracture zones, tends to be aseismic away from the transform faults according to global

earthquake catalogs. The addition of magma from the Ascension Hot Spot into the ridge is thought to cause the positive depth anomaly between 8°30′S to 10°00′S (Fig. 2) (Brozena, 1986) which corresponds to a gap in earthquakes from the global catalogs. This area could be truly aseismic, or the increase in heat flow limit earthquake magnitudes so that they are unlikely to be recorded in catalogs, such as the PDE. We specifically look for evidence of seismicity in this area.

Instrumentation

A very broadband seismographic station was installed near Butt Crater, Ascension Island by Project IDA of Scripps Institution of Oceanography as part of the Global Seismographic Network program managed by Incorporated Research Institutions for Seismology (IRIS). The station, ASCN, located at 7°56′S, 14°22′W, began routine operation on 9 October 1994. The station uses a Teledyne Brown KS54000 three-component seismometer capable of recording ground motions from a few milliHertz to about 5 Hz; the sensor is deployed in a 7-inch diameter, cased, dry borehole at 100 meters depth to minimize ground vibrations resulting from surface effects such as wind and barometric changes. Additionally, a three-component Streckeisen STS-2 seismometer is used to record higher frequency seismic waves (up to about 35 Hz) that can result from nearby earthquakes; this instrument is contained in a sealed canister fixed to a concrete pedestal and buried at about one meter depth. Analog outputs of the sensors are digitized by a high dynamic range analog-to-digital converter and the resulting data streams are digitally filtered and decimated to more useful sample rates. Data from the broadband borehole sensor are continuously recorded at 20 samples per second, 1 sample per second, and 0.1 sample per second; 100 samples per second data streams are created from the high-frequency STS-2 sensor, but are recorded only if triggered by a seismic event; the trigger threshold is adjustable. For this study the threshold is set to a sig-

nal-to-noise ratio of 5.5. Precise timing is provided by the Global Positioning System. Data are recorded on digital-audio tape (DAT), but can also be retrieved quickly from an internal data buffer over a dial-up communications circuit in the event of a significant earthquake. All data are processed and checked at the IDA Data Collection Center before being placed in the open archives of the IRIS Data Management System.

The hydrophone array is part of the Missile Impact Locating System (MILS) run by the U.S. Air Force (Palmer *et al.*, 1994). There are 12 Broad Ocean Area (BOA) hydrophones, five of which are recorded on a regular basis (Fig. 1). The instruments surround Ascension Island and are within 30 km of its shore except for one instrument that is about 100 km south of the island. These hydrophones are tethered to the seafloor and are located between 800 and 1600 meters depth. Most of the BOA hydrophones reside near the oceanic sound channel axis - an acoustic waveguide which is caused by a minimum in the speed of sound in water with depth. Because of this, the hydrophones not only record *P*- and *S*-phases, but also *T*-phases (earthquake energy that propagates in the ocean waveguide, e. g. Fig. 1). The hydrophones are continuously recorded at 120 samples per second, and have a low corner frequency of approximately 5 Hz. The BOA hydrophones along with the seismic station ASCN make a unique array for studying mid-ocean seismicity.

Earthquake Magnitudes and Distribution

Seismic data are analyzed over a period of 188 days, during which time 121 earthquakes triggered the data recorder. Of these earthquakes, 78 have discernible *P*, *S*, or *T*-phases (e. g. Fig. 1), and 41 of those have impulsive *P*- and *S*-arrivals with picking errors less than 0.1 seconds allowing for reliable distance estimates from *S* minus *P* times (the time interval between the *P*- and *S*-

arrivals) using an appropriate oceanic crustal model (Tolstoy, 1994). Most of the events occur at approximately 90 to 100 km from ASCN (Fig. 3a) which is the distance to the intersection of the MAR and the Ascension Fracture Zone.

Knowing the distances to the earthquakes, we can determine seismic magnitudes for the events. A local magnitude scale similar to Richter's local magnitude scale for California (Richter, 1935; Lay and Wallace, 1995) is used:

$$M_L = \log\left(\frac{A}{T}\right) + 3 \cdot \log(\Delta) - 4.2$$

where A is the maximum displacement of the S-wavetrain in microns, T is the average period of the signal in seconds, and Δ is the distance of the earthquake from ASCN in kilometers. The magnitude scale is calibrated with two earthquakes that have locations and magnitudes in the PDE catalog, but both of these events lie almost 10 degrees away, which is further from the seismic station than is usually used for local magnitudes. Because of this the magnitude scale may be systematically biased. Since there is only one seismic station recording per event the magnitude estimates may also be sensitive to focal mechanism orientation.

Earthquake magnitudes in this study range from 0.4 to 6.2, but most of the events recorded are between magnitude 1.5 and 2.5 (Fig. 3b). The b-value, which indicates the frequency of earthquakes of a certain magnitude relative to another magnitude, is computed by a least-squares analysis using a magnitude range from 1.5 to 2.5. We do not include magnitudes so small as to be below the threshold of detectability at the MAR (see below), and not so large that insufficient time has passed to give a good statistical measure of the frequency of occurrence. The b-value is deter-

mined to be 0.74. Because b-values can be as large as 1, we may be missing some of the smaller earthquakes, but a value as small as 0.67 is not uncommon (Lay and Wallace, 1995).

We expect that some earthquakes will be too small to discern from the background seismic noise, and the triggering algorithm will miss events with small signal-to-noise ratios since it is set to record only when this ratio is greater than 5.5. Thus the magnitude detection threshold increases with distance because of attenuation and geometrical spreading. A minimum observable magnitude function is computed from data which have reliable S minus P times. This function is used to determine the isograms in Fig. 2 which show the minimum magnitude earthquake observable at a given distance. The zero magnitude isogram is an extrapolation since we have no magnitudes below 0.4. At the MAR, where most of the seismicity originates, earthquakes as small as magnitude 1.7 are observable; that is almost 3 orders of magnitude smaller than seen in the PDE catalog for this area.

Earthquake Locations

Using the MILS hydrophone array and the ASCN seismic station together as an array or network we determine precise locations for six earthquakes (Table 1), two along the Ascension Fracture Zone (AFZ) and four at the ridge transform intersection. The USGS program HYPOELLIPSE (Lahr, 1993) is used to determine locations and 68% confidence error bounds. The depths are constrained to be less than 10 km, which is a commonly accepted depth for ridge seismicity (e. g. Toomey *et al.*, 1985, Huang and Solomon, 1988).

Two of the earthquakes occur on the AFZ just northwest of the island (Fig. 2b). These two events occur close to the array which allows for constraints not only on epicentral location but

also on depth. The earthquakes occur near one another on the south wall of the fracture zone. The earthquakes are shallow, about 1.5±1 km below the seafloor. The first earthquake, the main shock, has a local magnitude of 2.6, and the second earthquake, an aftershock, has a magnitude of 0.6 and happens two days after the first. These earthquakes are an example of the type of seismicity that is missed in the global catalogs, which in general show the AFZ as aseismic.

The other four earthquakes are located at the intersection of the MAR and the AFZ (Fig. 2a). Since the closest instrument is almost 100 km away, depth control is poor, and depths are fixed during location to be less than 10 km. The median valley of the MAR deepens into a hole as it approaches the transform fault at the north end of the ridge segment. All four epicenters are near or within this deep hole, but no PDE earthquakes from the last 7 years lie in this region. Instead, the PDE events cluster south of the transform on the edges of the median valley. The computed errors in our locations are less than 3 km for two events and around 10 km for the other two; the difference is due to whether or not the *P*-wave is visible at the hydrophone far to the south of Ascension Island. This station significantly increases the aperture of the array and thus the resolution of our locations. Although we are dealing with small numbers it seems more than coincidence that earthquakes recorded in the PDE catalog and the earthquakes presented here differ in location. Our array is west of the MAR and has limited azimuthal coverage, but the oceanic crust is relatively homogenous which diminishes systematic errors in locations compared to many land sites. In addition the ray paths used to calculate locations travel just below the crust-mantle boundary where seismic velocities only vary slightly. Also the distance to the earthquakes are determined from differential travel times which tends to minimize path dependent effects. It is known that the PDE locations in the North Atlantic are biased because of uneven instrument distribution (Bergman and Solomon, 1990), and the bias is likely to be similar in the South Atlantic.

For these reasons our locations are probably more accurate than the PDE locations. It is also possible that the larger earthquakes which are detected in the PDE do not occur on the faults at the transform-ridge intersection due to some inherent property of the crust (Wolfe *et al.*, 1993), such as a change in the brittle-ductile transition depth.

Regional Earthquakes

Although locations for regional earthquakes, 2 to 10 degrees away, are not calculated in this study, two sets of earthquakes are recorded and are interesting in their own right. The two main earthquakes in the first set occurred several months apart (Fig. 4), and are located near the south end of the aseismic region on the MAR at about 10°S - 250 km away from Ascension - and have magnitudes of about 5.0. The seismogram on top of Fig. 4 actually records a double event; two earthquakes separated by a few minutes. Both seismograms show large surface waves, but lack visible body waves that one would expect to see in the high-pass filtered data. Although these events are located in the PDE, which uses body waves for locations, the globally picked *P*-waves for at least the first event are few, and all are emergent signals. It is possible the lack of body-wave energy is due to a shadow zone created by upper-mantle structure (Lay and Wallace, 1995). An alternative explanation, based on the similarity of the seismograms to those of an unusual earthquake in the Santa Maria Basin, California observed by Kanamori and Hauksson, 1992, is that these events have anomalously slow energy release reducing the high-frequency content and emphasizing the surface waves. This slow energy release can occur at volcanic sites resulting in emergent body-wave arrivals (Malone, 1983), and may be the cause of the small *P*- and *S*-arrivals.

The second set of earthquakes (Fig. 5) occurred on a transform fault near the equator. The contrast of the seismograms to the first set is striking. In the top seismogram (magnitude 6.2) the *P*-,

S- and *T*-phases are clearly visible, as are the surface waves. The bottom seismogram shows a smaller earthquake with the same *T* minus *P* time which occurred several hours after the top event and is thus taken to be an aftershock. The aftershock lacks any clear *S*-arrival even though the signal-to-noise ratio of the *P*-wave is large enough that one would expect to see it. This same phenomenon is observed in other aftershocks as well. There is nothing unusual about the mainshock. It is clearly tectonic in origin because the strike-slip moment tensor from the Harvard Quick CMT database is consistent with the epicenter lying near a major transform fault. An obvious explanation for the lack of *S*-waves in the aftershocks is not apparent.

Discussion and Conclusions

The earthquakes observed in this study, which occur about every other day, all originate outside Ascension Island. There are a few unidentifiable seismic events, i. e., *P*- and *S*-waves could not be picked. These may be small, local events on the island either man-made or natural; or they could be smaller, more distant earthquakes with a low signal-to-noise ratio. A series of events we recorded have *S* minus *P* times of about 1.2 seconds which places them on the island, but these have been confirmed as ammunition detonations. We see no definite evidence for local (on Ascension Island) seismic activity of either tectonic or geothermal origin. This is different from current geothermal fields such as the Coso and Jemez Mountain Volcanic Fields, in California and New Mexico respectively, which exhibit active seismicity (e. g. Roquemore and Simila, 1994, Ankeny *et al.*, 1986).

Ridge seismicity we located does not coincide with PDE locations of previous earthquakes and is most likely due to the larger systematic mislocation errors of the PDE events. There is no direct evidence for seismicity on the shallow portion of the ridge which lacks earthquakes in the global

catalogs. Most of the earthquakes in this study are about 100 km away from ASCN, which is about the perpendicular distance to the ridge, but the aseismic portion of the ridge is further away. There are four events that are greater than 120 km away which could originate from this shallow ridge segment, but they more likely occur on the transform fault of the AFZ. The seismicity on this portion of the ridge will be better constrained when we incorporate data from another Global Seismographic Network station on St. Helena Island (1290 km to the southeast) installed in June 1995.

This is a preliminary study which shows that the ASCN seismic station can be used in conjunction with the MILS hydrophone array to study Mid-Atlantic Ridge seismicity and local microseismicity. Precise epicenter locations, with errors less than 10 km and frequently less than 3 km, are determined for both ridge and fracture zone earthquakes, and depths are constrained to a precision of 1 km for the latter. Because it is a permanent installation, this station has an advantage over previous ridge microseismicity studies which in general are short-term OBS deployments, although the OBS instruments have the advantage of being directly on the ridge. In addition, ASCN is a broadband station, something not yet common with ocean bottom instruments. With this broadband data it will be possible to determine more characteristics of some of the larger earthquakes, such as fault geometry and time functions of moment release, and with more earthquake recordings we will be able to compose a better picture of present day ridge seismicity and how it relates to ridge dynamics.

Acknowledgments

Data from the MILS hydrophone network were made available by the Air Force Technical Applications Center; we thank Frank Pilotte and Ellen Herron for their assistance in providing

this data. We thank David Palmer of NOAA/AMO Laboratory for providing information regarding the hydrophone network. This research was supported by Advance Research Projects Agency contract number MDA 972 91 C-005. The IDA Seismographic Network, an element of the IRIS Global Seismographic Network, is supported by Incorporated Research Institutions for Seismology subaward number 0162, the Cecil H. and Ida M. Green Foundation for Earth Sciences, and Scripps Institution of Oceanography. The seismographic station on Ascension Island is operated by the staff of the British Broadcasting Corporation.

Reference

Ankeny, L. A., Braile, L. W. and Olsen, K. H. (1986) Upper crustal structure beneath the Jemez Mountains Volcanic Field, New Mexico, determined by three-dimensional simultaneous inversion of seismic refraction and earthquake data. *J. Geophys. Res.* **91**, 6188-6198.

Atkins, F. B., Baker, P. E., Bell, J. D. and Smith, D. G. W. (1969) Oxford Expedition to Ascension Island. *Nature* **204**, 722-724.

Baker, P. E. (1973) Islands of the South Atlantic. *Ocean Basins Margins* **1**, 493-549.

Bergman, E. A. and Solomon, S. C. (1988) Transform fault earthquakes in the North Atlantic: source mechanisms and depth of faulting. *J. Geophys. Res.* **93**, 9027-9057.

Bergman, E. A. and Solomon, S. C. (1990) Earthquake swarms on the Mid-Atlantic Ridge: products of magmatism or extensional tectonics. *J. Geophys. Res.* **95**, 4943-4965.

Brozena, J. M. (1986) Temporal and Spatial Variability of seafloor spreading processes in the northern South Atlantic. *J. Geophys. Res.* **91**, 497-510.

Burke, K. C. and Wilson, J. T. (1976) Hot spots on the Earth's Surface. *Sci. Am.* **235**, 46-57.

Cande, S. C., LaBrecque, J. L. and Haxby, W. F. (1988) Plate kinematics of the South Atlantic: chron C34 to present. *J. Geophys. Res.* **93**, 13479-13492.

Huang, P. Y., Solomon, S. C., Bergman, E. A. and Nabelek, J. L. (1986) Focal depths and mechanisms of Mid-Atlantic Ridge earthquakes from body waveform inversion. *J. Geophys. Res.* **91**, 579-598.

Huang, P. Y. and Solomon, S. C. (1988) Centroid depths of mid-ocean ridge earthquakes: dependence on spreading rate. *J. Geophys. Res.* **93**, 13455-13477.

Kanamori, H. and Hauksson, E. (1992) A slow earthquake in the Santa Maria Basin, California. *Bull. Seism. Soc. Am* **82**, 2087-2096.

Lahr, J. (1993) HYPOELLIPSE: A computer program for determining local earthquake hypocentral parameters, magnitude, and first motion pattern. *USGS Open File Report 89-116.*

Lay, T. and Wallace, T. C. (1995) *Modern Global Seismology*, Academic Press, San Diego, 521-523.

Malone, S. D. (1983) Volcanic earthquakes: examples from Mount St. Helens. Earthquakes: Observation, Theory and Interpretation.

Morgan, W. J. (1971) Convection plumes in the lower mantle. *Nature* **230**, 42-43.

O'Connor, J. M. and le Roex, A. P. (1992) South Atlantic hot spot-plume systems: 1. distribution of volcanism in time and space. *Earth Planet. Sci. Lett.* **113**, 343-364.

Palmer, D. R., Georges, T. M., Wilson, J. J., Weiner, L. D., Paisleym J. A., Mathiesen, R., Pleshek, R. R. and Mabe, R. R. (1994) Reception at Ascension of the Heard Island Feasibility Test transmissions. *J. Acoust. Soc. Am.* **96**, 2432-2440.

Richter, C.F. (1935) An Instrumental Earthquake Magnitude Scale. *Bull. Seism. Soc. Am.* **25**, 1-32.

Romero, A. E. Jr., McEvilly, T. V., Majer, E. L. and Vasco, D. (1995) Characterization of the geothermal system beneath the northwest geysers steam field, California, from seismicity and velocity patterns. *Geothermics* **24**, 471-487.

Roquemore, G. R. and Simila, G. W. (1994) Aftershocks from the 28 June 1992 Landers earthquake: northern Mojave to the Coso volcanic field, California. *Bull. Seism. Soc. Am.* **84**, 854-862.

Tolstoy, M. (1994) A comparison of slow and fast spreading ridge axis structure from seismic data. Ph.D. Thesis, Institute of Geophysics and Planetary Physics, Scripps Institution of Oceanography, University of California San Diego.

Toomey, D. R., Solomon, S. C., Purdy, G. M. and Murray, M. H. (1985) Microearthquakes beneath the median valley of the Mid-Atlantic Ridge near 23°N: hypocenters and focal mechanisms. *J. Geophys. Res.* **90**, 5443-5458.

van Andel, Tj. H., Rea D. K., Von Herzen, R. P. and Hoskins H. (1973) Ascension Fracture Zone, Ascension Island, and the Mid-Atlantic Ridge. *Geol. Soc. America Bull.* **84**, 1527-1546.

Wolfe, C. J., Bergman, E. A. and Solomon, S. C. (1993) Oceanic transform earthquakes with unusual mechanisms or locations: relation to fault geometry and state of stress in the adjacent lithosphere. *J. Geophys. Res.* **98**, 16187-16211.

Figure Captions

Fig. 1. Location of Ascension Island and Global Seismographic Network station ASCN relative to the Mid-Atlantic Ridge and Ascension Fracture Zone. Also shown are locations of BOA hydrophones of the Missile Impact Locating System (MILS). Records from the MILS hydrophones (traces labeled "US") and seismic station ASCN are shown for a M_L=3.7 earthquake on the Mid-Atlantic Ridge. The *P*- and *S*-phases are seen on all the records, although the *S* is only picked on ASCN. The *T*-phase is seen on three of the hydrophones, and is not visible on ASCN or the hydrophone which is in the shadow of Ascension Island.

Fig. 2. (a). Location of seismic station ASCN on Ascension Island with MILS hydrophones. ASCN and MILS data are used to locate six small earthquakes, shown by their error ellipses. Also shown are isograms of the observable magnitude threshold estimated from ASCN data. PDE events from 1988-95 are shown as filled white circles against SEA BEAM bathymetry. (b). Detail of the area around Ascension Island showing bathymetry from the standard 5-minute global topography model, ETOPO5 (National Geophysical Data Center Data Announcement 86-MGG-07), of the AFZ with magnitude 0 and 1 detection isograms.

Fig. 3. (a). Histogram of number of earthquakes seen at ASCN over a 188-day period, versus distance inferred from *S-P* times. (b). Histogram of number of earthquakes seen at ASCN, over the same period, versus M_L calculated using *S*-wave amplitudes and a relation derived in this study.

Fig. 4. Raw broadband (left) and high-pass filtered (right) data from ASCN for two similar earthquakes on the MAR about 250 km away. The earthquakes are similar in that almost no

appreciable body wave energy is seen. The top seismogram contains two earthquakes for which only the larger has a location. The expected *P*- and *S*-arrival times are plotted for the two magnitude 5 earthquakes. At least part of the two bursts of energy seen in the top high-passed seismogram is due to the *T*-waves from the two earthquakes; this is confirmed with hydrophone data. The first arrival present in the lower seismogram is possibly the *S*-wave.

Fig. 5. Raw broadband (left) and high-pass filtered (right) data from ASCN for two earthquakes on 18 May 1995. The upper event was in the PDE catalog and occurred on a transform fault 1142 km north of ASCN. The lower event is not in the PDE catalog, but is presumed to be an aftershock because the *T*-*P* times seen in the filtered data are similar; however no *S*-phase is apparent.

TABLE 1. Locations of Local Earthquakes

Event	Date	Location	Depth (km)	68% error ellipse (km)	M_L
1	22 Dec 1994	7°45´S, 14°38´W	1.5 ± 0.8	0.5 × 0.9	2.6
2	25 Dec 1994	7°45´S, 14°38´W	2.0 ± 0.9	0.9 × 1.0	0.7
3	9 Nov 1994	7°15´S, 13°33´W	< 10	2.9 × 3.2	3.7
4	5 Dec 1994	7°25´S, 13°27´W	< 10	6.0 × 10	1.9
5	10 Dec 1994	7°22´S, 13°33´W	< 10	10 × 20	1.8
6	14 Dec 1994	7°35´S, 13°28´W	< 10	2.2 × 2.4	2.2

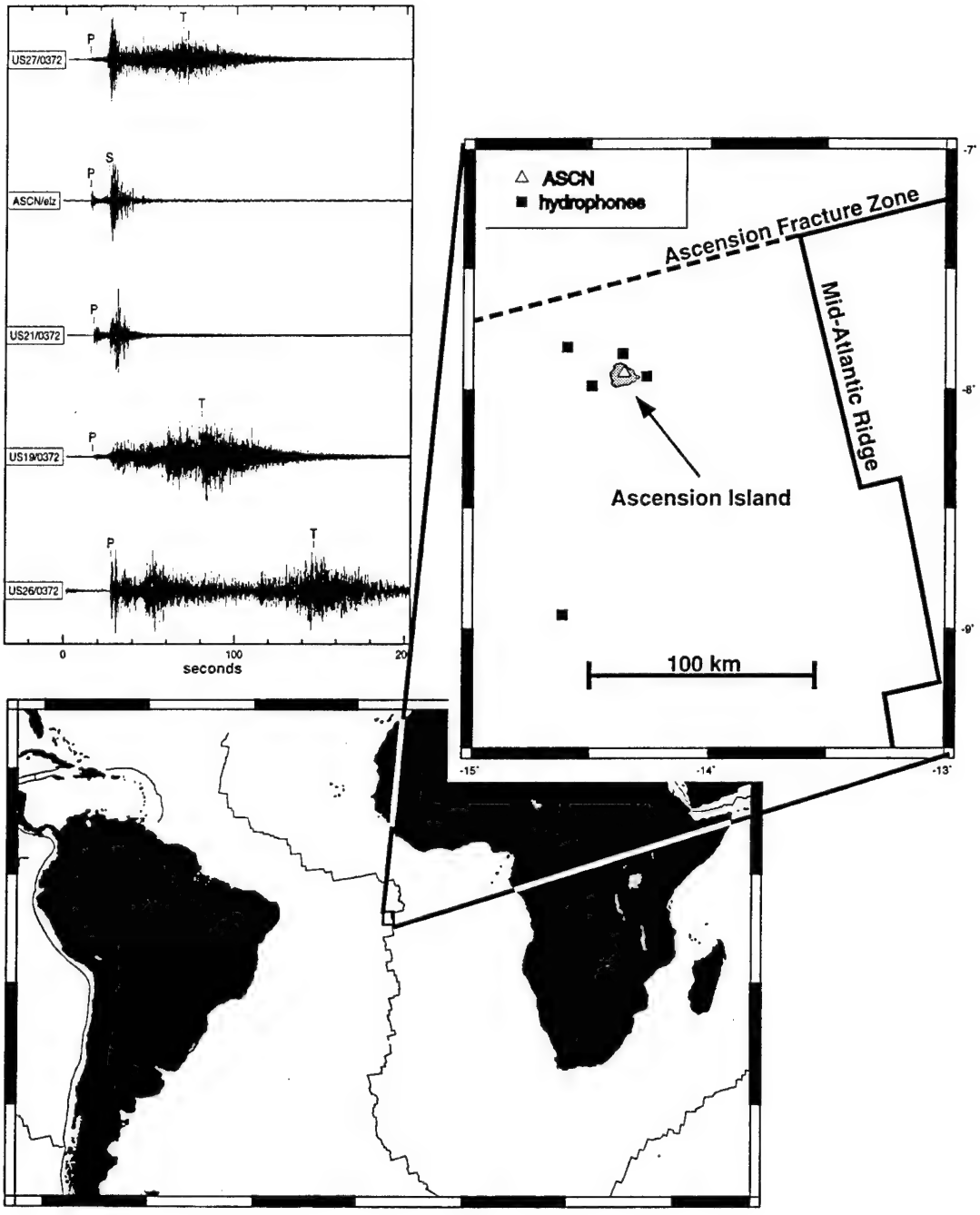
US27/0372
P
T
ASCN/elz
S
P
US21/0372
P
US19/0372
T
P
US26/0372
P
T
0
100
seconds
ASCN
hydrophones
Ascension Fracture Zone
Mid-Atlantic Ridge
Ascension Island
100 km
-7°
-8°
-9°
-15°
-14°
-13°

Figure 1

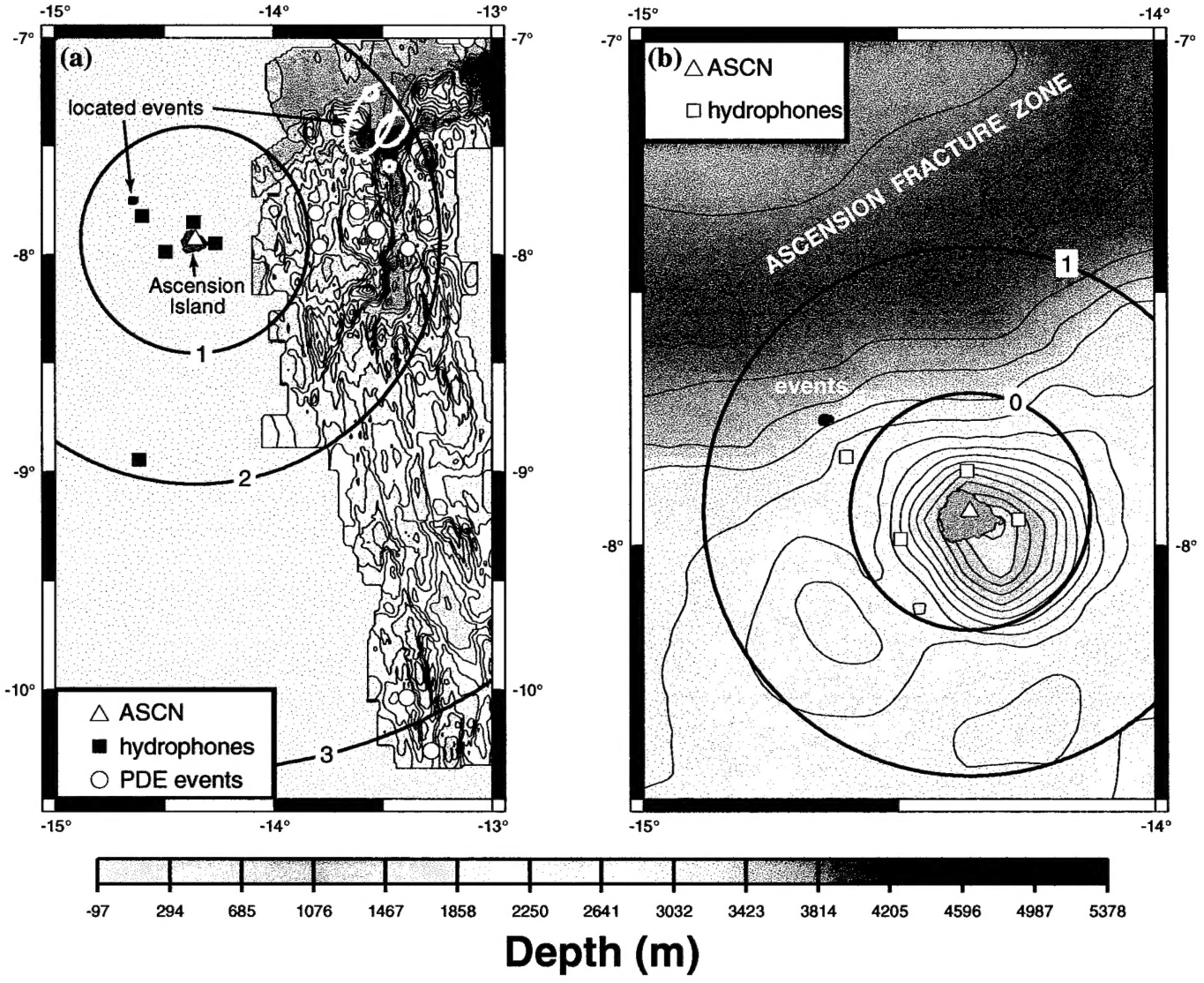
(a)
located events
Ascension Island
1
2
3
△ ASCN
■ hydrophones
○ PDE events
(b) △ ASCN
□ hydrophones
ASCENSION FRACTURE ZONE
events
0
1
-15°
-14°
-13°
-7°
-8°
-9°
-10°
-97
294
685
1076
1467
1858
2250
2641
3032
3423
3814
4205
4596
4987
5378
Depth (m)

Figure 2

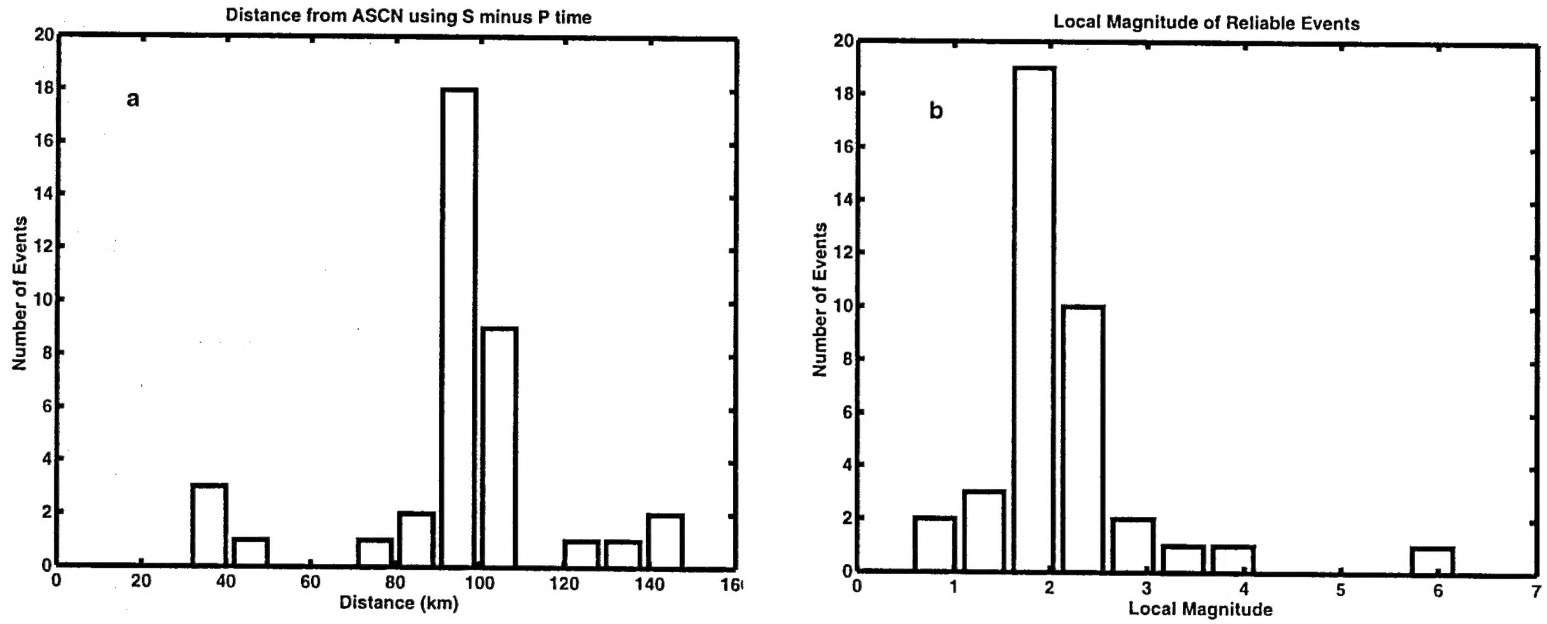
Distance from ASCN using S minus P time
a
Number of Events
Distance (km)
0
20
40
60
80
100
120
140
Local Magnitude of Reliable Events
b
Number of Events
Local Magnitude
0
1
2
3
4
5
6
7

Figure 3

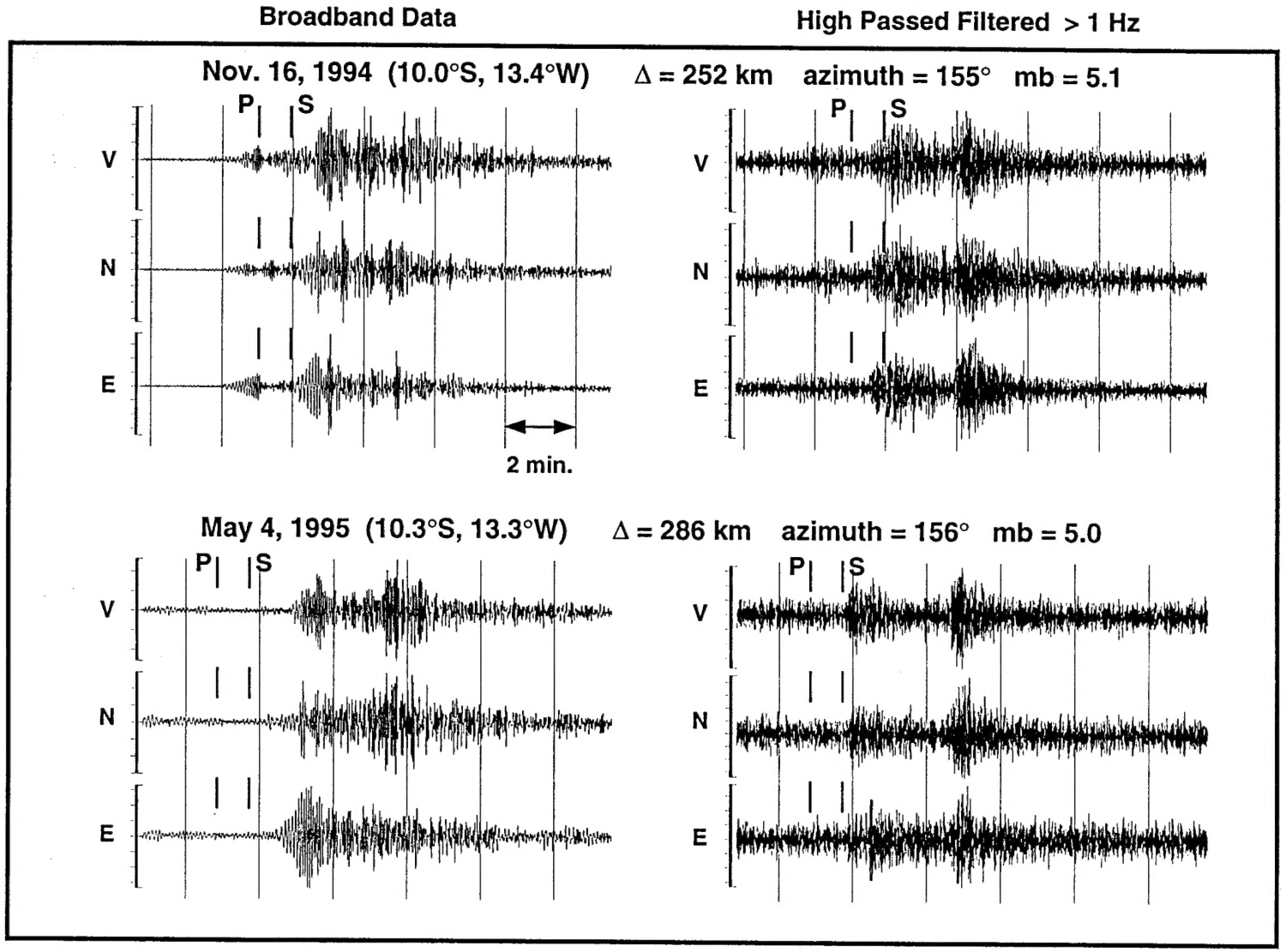
Broadband Data
High Passed Filtered > 1 Hz
Nov. 16, 1994 (10.0°S, 13.4°W) Δ = 252 km azimuth = 155° mb = 5.1
P
S
V
N
E
2 min.
May 4, 1995 (10.3°S, 13.3°W) Δ = 286 km azimuth = 156° mb = 5.0

Figure 4

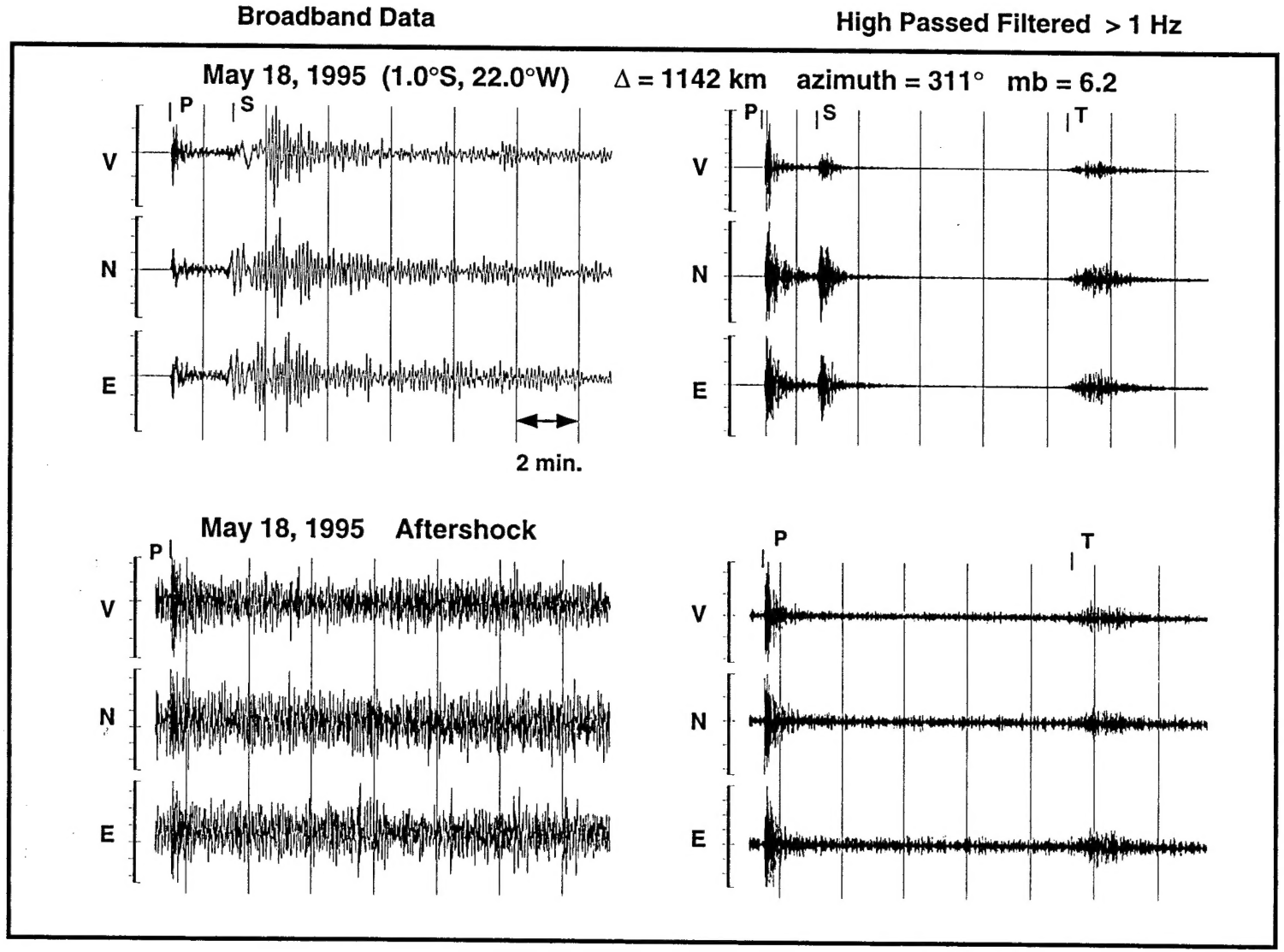
Broadband Data
High Passed Filtered > 1 Hz
May 18, 1995 (1.0°S, 22.0°W) Δ = 1142 km azimuth = 311° mb = 6.2
P
S
T
V
N
E
2 min.
May 18, 1995 Aftershock

Figure 5